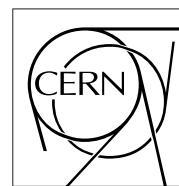


The Compact Muon Solenoid Experiment

# CMS Note

Mailing address: CMS CERN, CH-1211 GENEVA 23, Switzerland



15 March 1999

## Untagged analysis of $B_s^0 \rightarrow J/\psi\phi$ channel

François Charles <sup>a)</sup>

*Groupe de Recherche en Physique des Hautes Energies  
Université de Haute Alsace, 61 rue A. Camus 68093 Mulhouse, France*

### Abstract

We have studied the  $B_s^0 \rightarrow J/\psi\phi$  channel using a transversity analysis. We show that CMS will be able to separate the Light and Heavy eigenstates of  $B_s^0$  and to measure their lifetime. Consequently we expect to measure  $x_s$  indirectly for any value beyond the present experimental lower limit. Fitting a multiangle distribution we also expect to put an upper limit :  $\lambda^2\eta < 0.15$  for  $\Delta\Gamma = 0.2$

---

<sup>a)</sup> Email: charles@sbghp3.in2p3.fr

# 1 Introduction

The  $B_s^0 \rightarrow J/\psi\phi$  channel is one of the gold plated channel for the LHC experiments as it presents several advantages. First of all, through the  $J/\psi$  decay one can expect to have an excellent trigger either in dimuon or dielectron production at the first and second level. Secondly, it is a very clean channel due to the three resonances  $J/\psi$ ,  $B_s^0$ , and the extremely narrow  $\phi$ . On the other hand, the CP violation effect in this channel is expected to be very small :  $A_{CP} \propto \sin 2\Phi$  (with  $\Phi = O(0.03)$  ).

The  $B_s^0$  and  $\bar{B}_s^0$  meson are expected to mix (see figure 1) and appear as two mass eigenstates:  $B_s^L$  light and  $B_s^H$  heavy (similarly to the  $K^0$  system). The particle-antiparticle mixing accounts for the mass difference in the neutral B meson system and this process is a Flavour Changing Neutral Current and related to the CP violation.

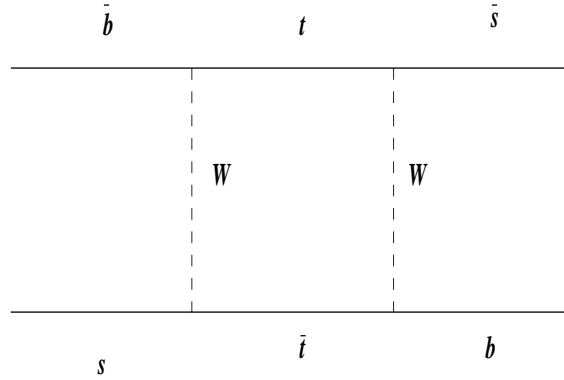


Figure 1: strange B meson oscillation diagram

To a good approximation CP violation can be neglected in determining the masses and the mass eigenstates correspond to the CP eigenstates with  $B_s^L$  being CP even and  $B_s^H$  CP odd. To observe experimentally the  $B_s$  oscillation one usually tag the  $B_s$  at the production and decay. This method considerably reduces the number of observed events. In the following we propose to use an untagged distribution. The lifetime difference of the two CP states has been calculated using heavy quark expansion :  $\frac{\delta\Gamma}{\Gamma} = 0.16 \pm 0.1$  [1] . It updates an explicit calculation [4] which wrote

$$\Delta\Gamma \simeq 0.18 \frac{f_{B_s^0}^2}{(200MeV)^2}$$

Lattice calculations give for the light decay constant  $f_{B_s^0} = 181 \pm 36MeV$  [2]. It is expected that an accuracy of 10% on this number could be reached assuming some progress in lattice calculations. The ratio of the mass splitting to the width difference of strange B meson is predicted to be large . To the lowest order and neglecting QCD corrections which may be important:

$$\frac{|\Delta m|}{\Delta\Gamma} = \frac{2}{3\pi} \frac{m_t^2 h(m_t^2/M_W^2)}{m_b^2} \left(1 - \frac{8}{3} \frac{m_c^2}{m_b^2}\right)^{-1} = 178.6 \pm 83$$

where  $h(x)$  decreases monotonically from 1 at  $x=0$  to  $1/4$  at  $x \rightarrow \infty$ . It is about 0.54 for  $m_t = 180 GeV/c^2$ . So we can deduce (neglecting the uncertainty on this ratio):

$$\Delta m \simeq 178.6(\Gamma_L - \Gamma_H) \Rightarrow x_s \simeq 178.6 \frac{\Delta\Gamma}{\Gamma}$$

We thus can access  $x_s$  by separating the CP eigenstates and measuring their lifetime. This method should prove to be efficient for large  $x_s$  where the lifetime difference is expected to be large. In that sense the LEP/CDF/SLD combined limit:  $\delta m_s > 12.4ps^{-1}$  [3] is encouraging. To separate the  $B_s^0$  state we have used the following method. The  $B_s^0$  meson is spinless, so its decay product polarization :  $J/\psi$  and  $\phi$  which are both vector will be of course

correlated. We can express the amplitude in the following way [5, 6] :

$$A(B_s^0 \rightarrow J/\psi\phi) = \frac{A_0(t)}{x} \epsilon_{J/\psi}^{*L} \epsilon_\phi^{*L} - A_{||}(t) \epsilon_{J/\psi}^{*T} \epsilon_\phi^{*T} / \sqrt{2} - i A_\perp(t) \epsilon_{J/\psi}^* \times \epsilon_\phi^* p_\phi / \sqrt{2}$$

where  $A_0$  is the amplitude for which the linear polarization states of the vector meson are longitudinal to their directions of motion, while  $A_{||}$  and  $A_\perp$  are transverse to their direction of motion and respectively parallel or perpendicular to each other.  $\epsilon_{J/\psi}^{*T}$  represent the polarization vector of the vector  $J/\psi$ . The two CP even decay amplitude are  $A_0$  and  $A_{||}$  while  $A_\perp$  is CP odd.

In this specific frame the decay width is defined as

$$d\Gamma(B_s^0 \rightarrow J/\psi\phi)/dt = |A_0|^2 + |A_{||}|^2 + |A_\perp|^2$$

In the following, one use a frame [5, 6] to define a transverse variable (see figure 2).

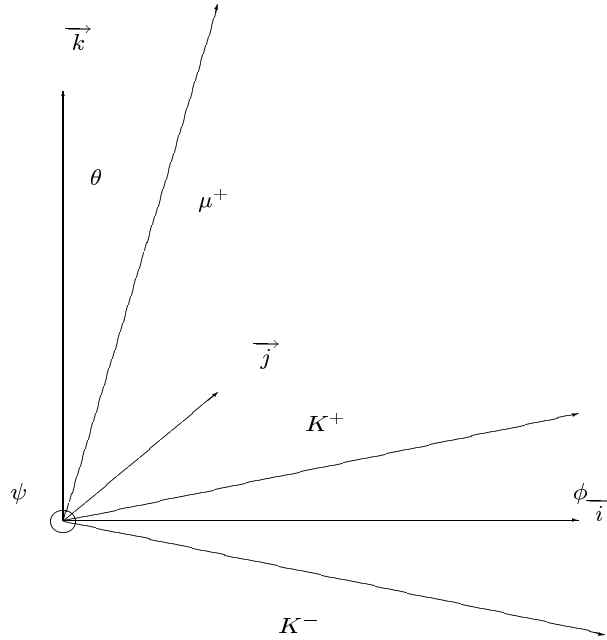


Figure 2: Transversity analysis frame

In the  $J/\psi$  restframe we define:  $\vec{i}$  as the  $\phi$  direction,  $\vec{j}$  as orthogonal to  $\vec{i}$  in the  $(K^+, K^-)$  plane with  $p_y(K^+) > 0$ ,  $\vec{k} = \vec{i} \wedge \vec{j}$ ,  $\theta$  as the angle between  $\vec{k}$  and  $\vec{p}(\mu^+)$ ,  $\Phi$  being the angle between the  $l^+$  projection in the  $\vec{i}, \vec{j}$  plane and the  $\vec{i}$  direction.  $\psi$  is defined as the angle of  $K^+$  in the  $\phi$  restframe with the helicity axis (the negative direction of the  $J/\psi$  in that frame).

Finally one obtain the following differential distribution [9, 8] :

$$d^4\Gamma(B_s^0 \rightarrow J/\psi\phi)/dt = \frac{9}{16\pi} [2|A_0(0)|^2 e^{-\Gamma_L t} \cos^2\psi (1 - \sin^2\theta \cos^2\Phi) + \sin^2\psi (|A_{||}(0)|^2 e^{-\Gamma_L t} (1 - \sin^2\theta \sin^2\Phi) + |A_\perp(0)|^2 e^{-\Gamma_H t} \sin^2\theta) + \frac{1}{\sqrt{2}} |A_0(0)| |A_{||}(0)| \cos(\delta_2 - \delta_1) e^{-\Gamma_L t} \sin^2\theta \sin 2\Phi + (\frac{1}{\sqrt{2}} |A_0(0)| |A_\perp(0)| \cos\delta_2 \sin 2\psi \sin 2\theta \cos\Phi - |A_{||}(0)| |A_\perp(0)| \cos\delta_1 \sin^2\psi \sin 2\theta \sin\Phi) \frac{1}{2} (e^{-\Gamma_H t} - e^{-\Gamma_L t}) \delta\Phi_{ts}]$$

(1)

where  $\delta\Phi_{ts} = \arg(V_{cs}^*V_{cb}) - \arg(V_{ts}^*V_{tb})$ . At leading order in the Wolfenstein [7] expansion this phase vanishes. In the unitarity triangle we have :  $\delta\Phi_{ts} = \lambda^2\eta = O(0.03)$ . Determining the quantity  $\eta$  constraints the  $\gamma$  angle of the CKM matrix as :  $\sin\gamma = \frac{\eta}{R_b}$  where  $R_b = \frac{1}{\lambda} \frac{|V_{ub}|}{|V_{cb}|}$  ( $R_b = 0.36 \pm 0.08$  ). If we integrate equation (1) over  $\Phi$  and  $\psi$  we obtain the following equation:

$$\frac{d^2\Gamma}{d\cos\theta dt} = \frac{3}{8}p(t) * (1 + \cos^2\theta) + \frac{3}{4}m(t) * (1 - \cos^2\theta)$$

where  $p(t) = p(0)e^{-\Gamma_L t}$  is CP even and  $m(t) = m(0)e^{-\Gamma_H t}$  is CP odd.

We can observe on figure 3 the respective distribution of the light and heavy states for the  $\cos\theta$  variable for one year at low luminosity after selection.

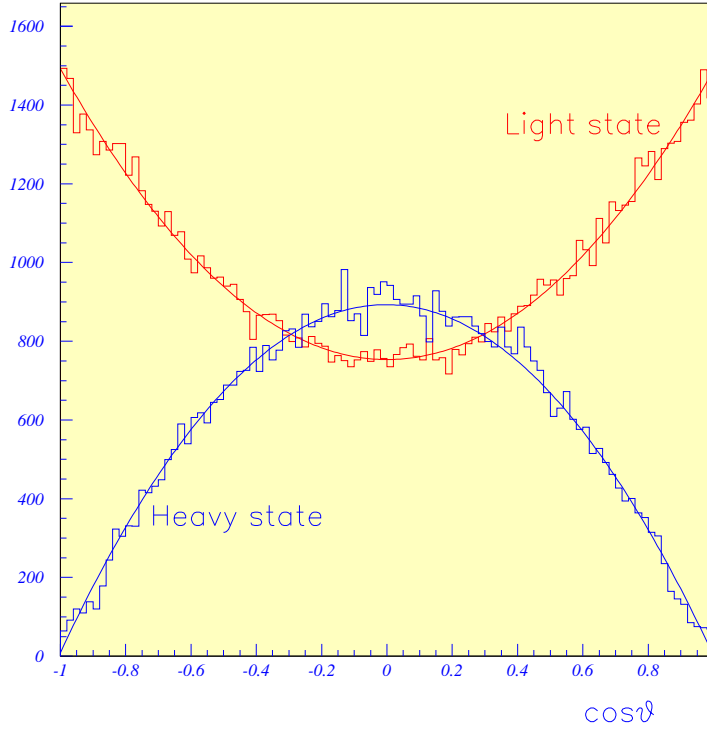


Figure 3: Light and heavy state angular distribution

In [10] we have used a very simple method to separate the two CP states. This was done in the following way:

$$E(t) = \int_{0.5}^{-0.5} \frac{d^2\Gamma}{d\cos\theta dt} d\cos\theta = \frac{13}{32}p(t) + \frac{11}{16}m(t)$$

$$P(t) = \left( \int_{-1}^{-0.5} + \int_{0.5}^1 \right) \frac{d^2\Gamma}{d\cos\theta dt} d\cos\theta = \frac{19}{32}p(t) + \frac{5}{16}m(t)$$

So we finally extract :

$$p(t) \propto \frac{d\Gamma}{dt} + \frac{8}{3}(P - E) \text{ and } m(t) \propto \frac{d\Gamma}{dt} - \frac{16}{3}(P - E)$$

## 2 Tools and assumptions

We assume the following value for the branching ratio:

$$BR(B_s^0 \rightarrow J/\psi\phi) = 1 \times 10^{-3}$$

compatible with the CDF value [11] :

$$B(B_s^0 \rightarrow J/\psi\phi) = 0.93 \pm 0.28 \pm 0.10 \pm 0.14 \times 10^{-3}$$

The CDF experiment also measured the polarization for the  $B_s^0 \rightarrow J/\psi\phi$  channel [12] . Their results are  $\Gamma_L/\Gamma = 0.56 \pm 0.21$  which correspond to  $|A_0(0)|^2 + |A_{||}(0)|^2 = 0.56$  . For this study Pythia 5.7 [13] has been used for the generation with CTEQ2L structure function while the tracking simulation was based on a parametrisation of the momentum resolution and on a Geant [14] description of the secondary vertex resolution.

### 3 Selection

We impose the following selection to obtain the signal events for the channel  $B_s^0 \rightarrow J/\psi\phi \rightarrow \mu^+\mu^-K^+K^-$  : we require the hadrons to be in the range  $|\eta| < 2.4$  with  $p_t^{had.} > 2 \text{ GeV}/c$ .

The muons are expected to fullfill the low  $p_t$  two muon trigger criteria:

$$\begin{array}{ll} p_t > 4.5 \text{ GeV}/c & 0.0 < |\eta| < 1.5 \\ p_t > 3.6 \text{ GeV}/c & 1.5 < |\eta| < 2.0 \\ p_t > 2.6 \text{ GeV}/c & 2.0 < |\eta| < 2.4 \end{array}$$

The invariant mass of the  $\mu$  pair (respectively  $K$  pair) and all four particles should be reconstructed in the window  $\Delta m < \pm 2\sigma_m$  of the  $J/\psi$  (respectively  $\phi$  and  $B_s^0$ ). The decay time should be  $t_{B_s^0} > 0.2 \text{ ps}$ . A good vertex is required:  $\chi_{\mu^+\mu^-K^+K^-}^2 < 5$ .

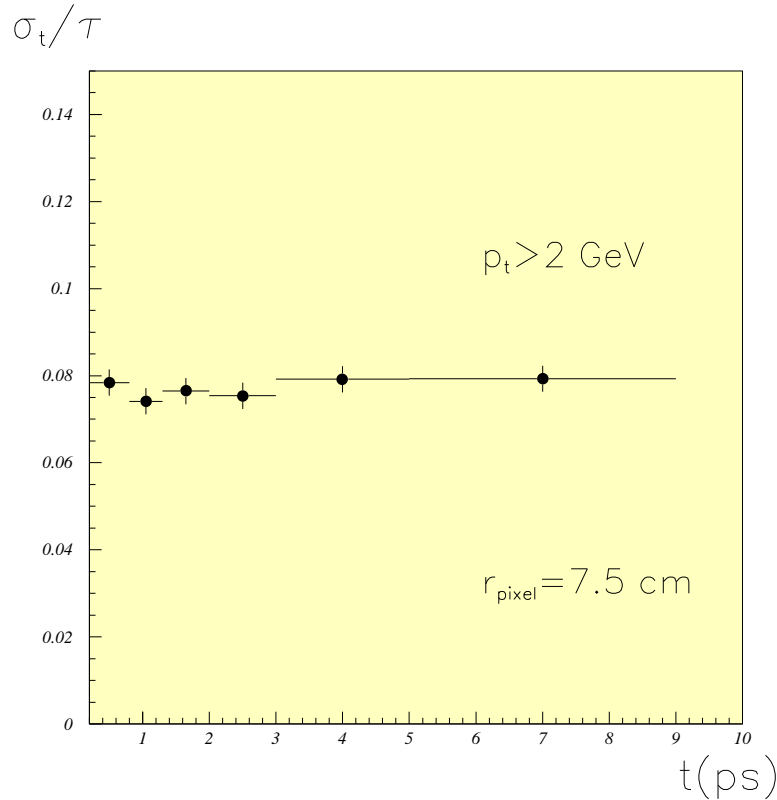


Figure 4: Time resolution for a four tracks secondary vertex reconstruction

The expected four tracks vertex time resolution can be evaluated on figure 4 for the  $B_s^0$  decay with  $p_t^{had.} > 2$  GeV/c and the muons passing the trigger requirement. It shows a very good resolution, stable with respect to the time. We also impose a vertex pointing cut:  $\Delta\alpha < 0.1$  rad, see figure 5.

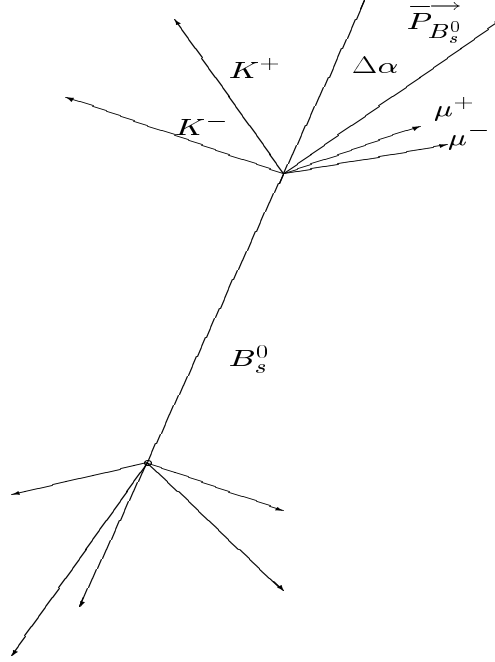


Figure 5:  $B_s^0 \rightarrow J/\psi\phi \rightarrow \mu^+\mu^-K^+K^-$  decay geometry

For an integrated luminosity of  $10^4$   $pb^{-1}$  we retain approximately 150000 signal events (we assume  $B(B_s^0 \rightarrow J/\psi\phi) = 10^{-3}$  [9]) while the background is kept at about 1%. The dominant background for this channel is  $B \rightarrow J/\psi(\rightarrow \mu^+\mu^-) + X$ . It is efficiently cut out by the strong requirements that were applied. We see on figure 6 the mass resolution for  $J/\psi$ ,  $\phi$  and  $B_s^0$  (the last one with background included), showing an excellent precision.

## 4 $x_s$ measurement

The effect of the selection on the considered variables can be appreciated on figure 7 and 8 showing the efficiency to be independent of  $\cos\theta$  and  $t$  variable within the statistical errors. Figure 9 illustrates the  $x_s$  measurement in the range 10 to 50. It shows a good agreement between the generated and the reconstructed value and doesn't degrade at high  $x_s$ , allowing a complete coverage of the range allowed by Standard Model and even beyond.

## 5 Multiangular fit

In order to extract the phase  $\delta\Phi_{ts}$  we have been attempting to fit the differential multiangular distribution. We have produced a number of events corresponding to an integrated luminosity of  $10^4 pb^{-1}$  i.e. 150000 events with the expected differential distribution for each variable (eq. 1). A gaussian smearing has been applied on the angular distribution according to the expected experimental one, see figure 10.

We can see on the next figure (11) the expected distribution for each variable. A loglikelihood fit was then attempted using Minuit [15]. This was performed for various values of the parameters (in agreement with the experimental constraints and the theoretical expectations). The 6 parameters  $A_0, A_{||}, \delta\Phi_{ts}, \delta_1, \delta_2, \Delta\Gamma$  of equation 1 were left free. Once convergence occurred, all parameters except  $\delta\Phi_{ts}$  were fixed and a new fit was performed in order to extract  $\delta\Phi_{ts}$ . Table 1 shows the expected errors for the parameters for one year at low luminosity of the

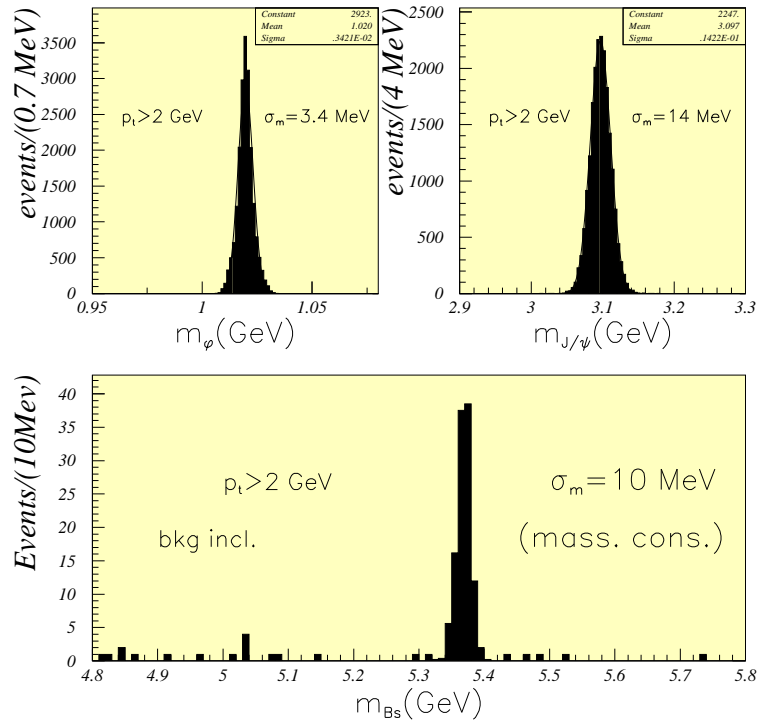


Figure 6: Mass resolutions for  $B_s^0 \rightarrow J/\psi \phi \rightarrow \mu^+ \mu^- K^+ K^-$

efficiency

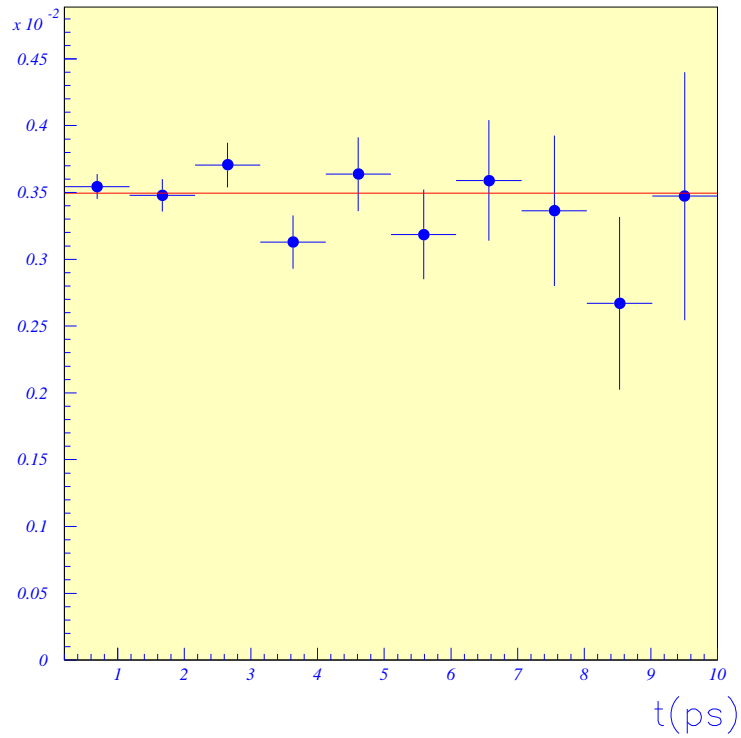


Figure 7: Efficiency of the selection

efficiency

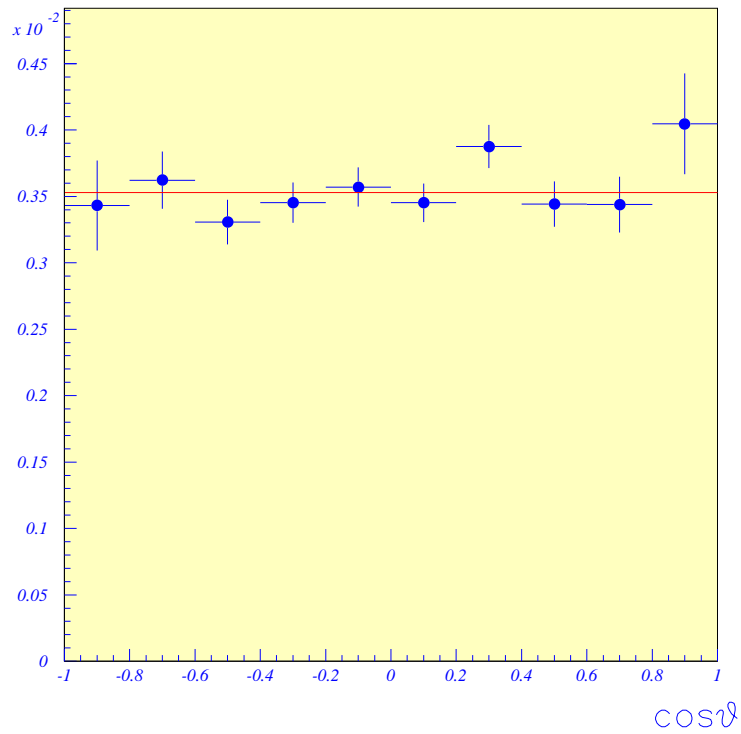


Figure 8: Efficiency of the selection

measured  $x_s$

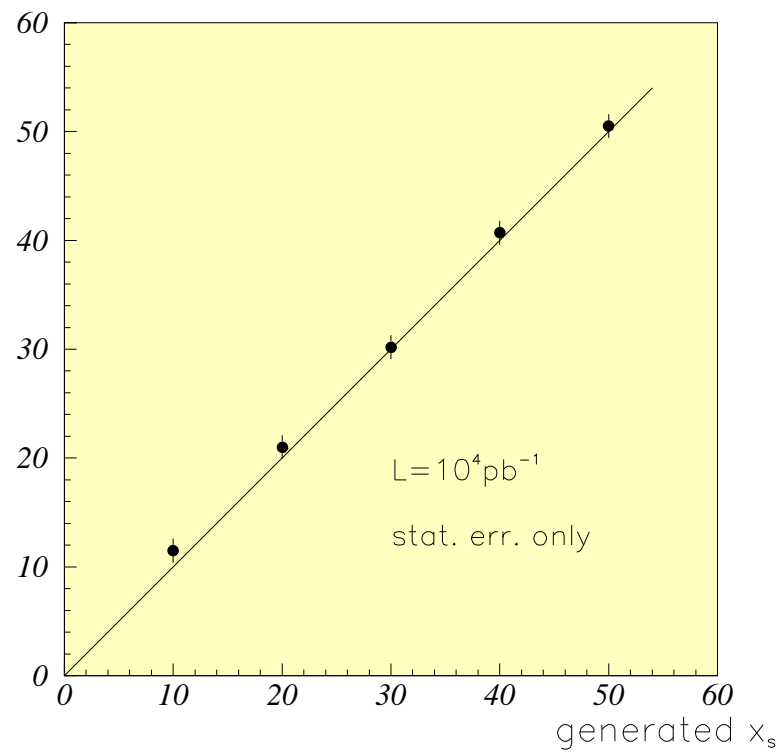


Figure 9: Indirect measurement of  $x_s$

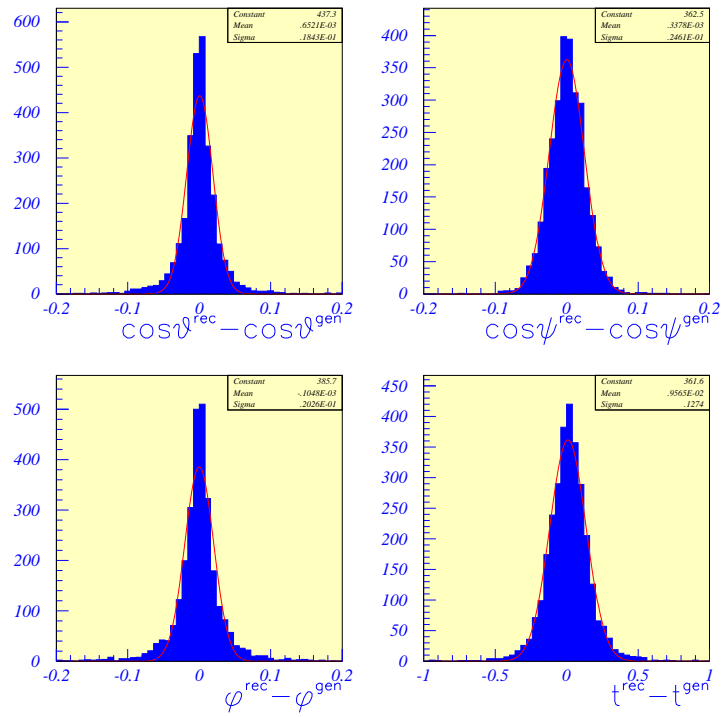


Figure 10: Angular resolution

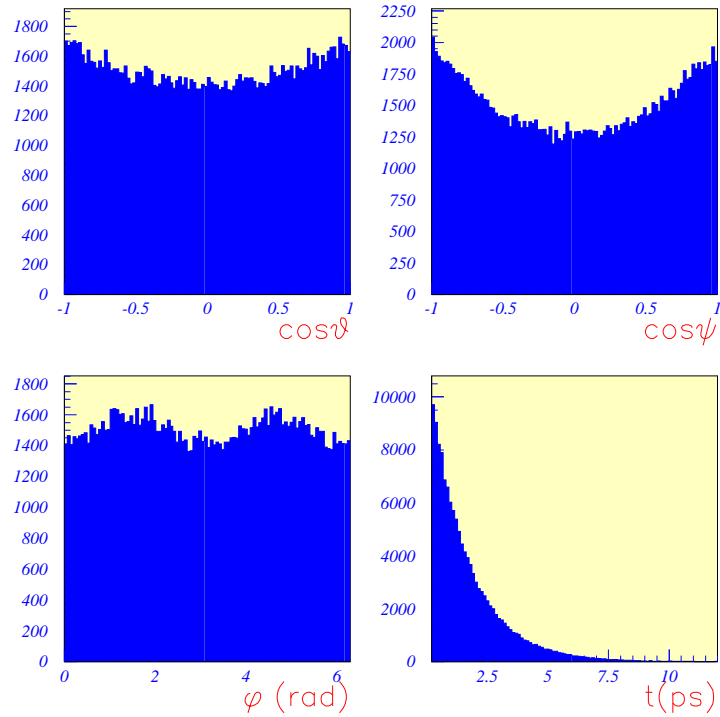


Figure 11: Angular distribution

LHC.

Parameter	$\frac{\delta A_0}{A_0}$	$\frac{\delta A_{  }}{A_{  }}$	$\frac{\delta \Delta\Gamma}{\Delta\Gamma}$	$\sigma(\delta\Phi_{ts})$	$\frac{\sigma(\delta_1)}{\delta_1}$	$\frac{\sigma(\delta_2)}{\pi-\delta_2}$
$\Delta\Gamma = 0.1$	0.4%	0.6%	5%	0.056	0.2%	4%
$\Delta\Gamma = 0.15$	0.4%	0.6%	4%	0.05	0.2%	4%
$\Delta\Gamma = 0.2$	0.4%	0.6%	3%	0.045	0.2%	4%

Table 1: Expected parameter error for  $L = 10^4 pb^{-1}$

Among the 6 parameters, 4 of them ( $A_0, A_{||}, \delta_1, \delta_2$ ) can be easily determined, the last 2 parameters  $\Delta\Gamma$  and  $\delta\Phi_{ts}$  have the largest relative error. The starting values of the parameters were  $A_0 = 0.52$ ,  $A_{||} = 0.445$ ,  $\delta\Phi_{ts} = 0.03$ ,  $\delta_1 = \pi$ ,  $\delta_2 = 0$ .

## 6 Conclusion and perspective

To summarize our results, we show that CMS will be able to measure the lifetime difference of the heavy and light mass eigenstates ( $\Delta\Gamma$ ) over the whole theoretical expected range and beyond. We thus expect to measure indirectly  $x_s$  for any possible value. This method will prove to be critical for values of  $x_s$  equal or above 50 where no other method can be used.

The transverse analysis of this channel will also provide us with the polarization factor and finally will give some constraints on the value of  $\delta\Phi_{ts}$ .  $B_s^0 \rightarrow J/\psi\phi$  will clearly be one of the most interesting channel for B physics at the LHC collider. One should note that a similar analysis can be performed for the channel  $B_d^0 \rightarrow J/\psi K^*$ .

### ACKNOWLEDGEMENTS

I would like to thank C. Racca and Y. Lemoigne for reading the manuscript.

## References

- [1] M.Beneke et al. SLAC-PUB-7165 (1996)
- [2] The MILC Collaboration Nucl.Phys.Proc.Suppl. 53 (1997) 358-361
- [3] Combined Results.. LEPBOSC
- [4] M. B. Voloshin Yad. Fiz. 46 (1987) 181
- [5] A. Dighe hep-ph/9511363
- [6] J. Rosner ,Phys Rev. D 42 (1990) 3732
- [7] L.Wolfenstein, Phys. Rev. Lett. 51 (1983) 1945
- [8] R. Fleischer Fermilab-PUB-96/079-T
- [9] A.Dighe et al. CERN-TH/98-85 (1998)
- [10] F.Charles Nucl. Phys. B (Proc. Suppl.) 55A (1997)
- [11] CDF coll. Fermilab-PUB-96/119-E
- [12] CDF coll. Fermilab-PUB-95/270-E
- [13] T.Sjostrand, Computer Phys. Comm. 82 (1994) 74.
- [14] CERN Prog. Lib. Long Writeup W5013
- [15] CERN Prog. Lib. Long Writeup D506